Proceedings of the 9th International Conference on Fluid Flow, Heat and Mass Transfer (FFHMT'22)
Niagara Falls, Canada – June 08-10, 2022
Paper No. 117
DOI: 10.11159/ffhmt22.117

Calculation of the Pressure Field around a Spherical-Cap Bubble

Abdullah Abbas Kendoush
Department of Nuclear Engineering Technology Augusta Technical College, Augusta, GA 30906, USA
akendoush@augustatech.edu

Abstract - The pressure field around a spherical-cap bubble was divided into a spherical frontal and a wake region. The pressure field in each region was derived from the equation of motion. Due to the almost flat base of the bubble, the flow field of the wake was considered similar to that behind a circular disk. The calculated pressure distribution revealed the phenomenon of the bubble skirt. The predicted pressure field of the spherical-cap bubble agreed well with the available experimental and theoretical results.
***Keywords*:** Two-phase flow, Spherical-cap bubble, Bubbly flow, Pressure Distribution,

1. Introduction

Spherical-cap bubbles are the last stage in evolution of the shapes of bubbles. Small bubbles start rising in spherical form then they deform into ellipsoidal shape due to the predominance of the inertia forces over the surface tension forces until they reach the spherical-cap shape which is shown in Fig. 1.

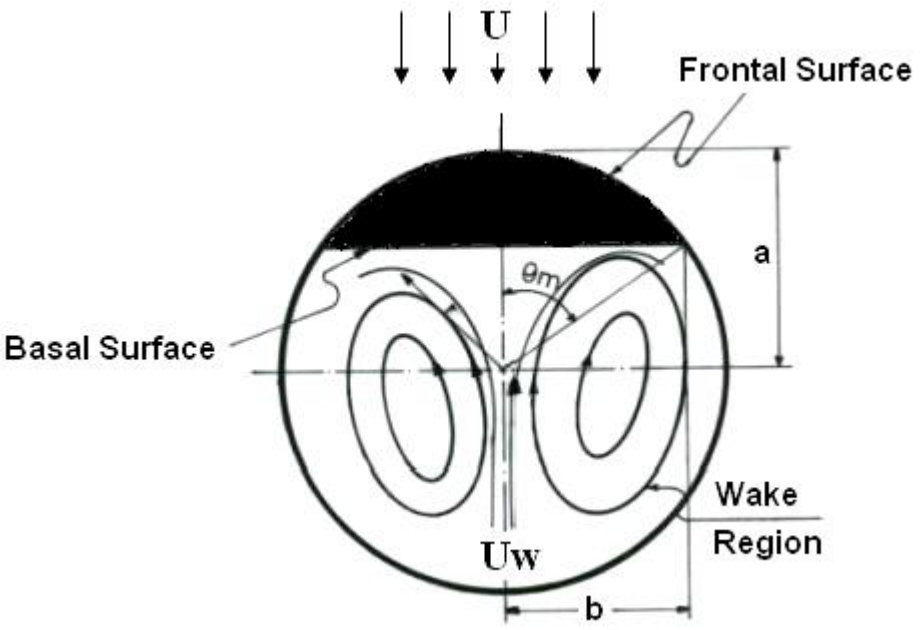

Fig. 1: Geometry of the spherical-cap bubble.

Past research of spherical-cap bubbles have dealt primarily with determining the drag forces, rate of rise and thermal convection (e.g. Wegener and Parlange [1]; Kendoush [2]; Maxworthy et al. [3]). The research of the pressure field around the spherical – cap bubble is rather limited.

Collins [4] proposed a model for the pressure distribution around the bubble by application of Bernoulli's equation to a streamline on the bubble surface. This model was confined to the spherical frontal region of the bubble and does not cover the wake region.

Lazarek and Littman [5] measured the pressure field around a circularly-capped air bubble which represents the two-dimensional version of the spherical-cap bubble. This type of bubbles is normally found in a narrow rectangular cross-section water column. They also analyzed the frontal pressure field by using an irrotational flow model on an oval body. The effects of the finite distance between the bounding walls of the column were accounted for by infinite reflections of the source and sink using the method of images.

In this paper detailed calculation of the entire pressure field, including the wake region of the spherical-cap bubble is presented, based on the solution of the equation of motion.

2. THE FRONTAL SURFACE OF THE BUBBLE

The flow field around the spherical-cap bubble is divided into two distinct regions as was done by Kendoush [2] in analyzing the rates of heat and mass transfer from the surface of the spherical-cap bubble. The first region is the frontal where the upstream surface of the bubble forms a portion of a sphere so the flow in this region resembles that around the sphere. The second is the wake region where the bubble has an almost flat base and the flow is approximated by that in the wake of a circular disk as shown in Fig. 2.

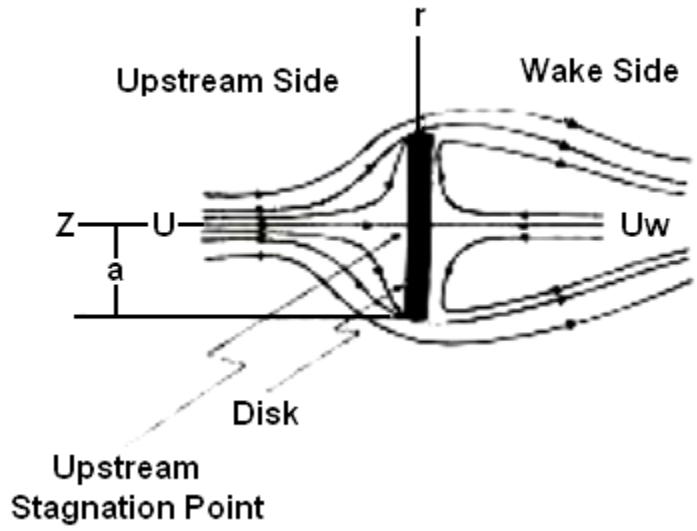

Fig. 2: The flow field around the circular disk.

The stream function Ψ for the inviscid irrotational flow around the spherical frontal surface is given as follows (Milne-Thomson [6], p. 488)

$$\Psi = 0.5U\{1-(a/r)^3\}(r\sin\theta)^2 \tag{1}$$

where U is the uniform fluid velocity at infinity , a is the radius of curvature of the spherical-cap bubble , r and θ are the polar coordinates. It is possible to calculate the velocity components V_r and V_θ of the main flow from the following equation (written in vector form)

$$(V_r, V_\theta) = -\nabla \psi \tag{2}$$

which gives

$$V_r = -U\cos\theta\left(1-\left[\frac{a}{r}\right]^3\right) \tag{3}$$

and

$$V_\theta = U\sin\theta\left(1+0.5\left[\frac{a}{r}\right]^3\right) \tag{4}$$

The equation of motion for the axisymmetric flow in spherical coordinates is

$$\rho\left(V_r\frac{\partial V_r}{\partial r}+\frac{V_\theta}{r}\frac{\partial V_r}{\partial \theta}-\frac{{V_\theta}^2}{r}\right) = -\frac{\partial P}{\partial r}+\mu\left(\nabla^2 V_r-\frac{2V_r}{r^2}-\frac{2}{r^2}\frac{\partial V_\theta}{\partial \theta}-\frac{2V_\theta\cot\theta}{r^2}\right) \tag{5}$$

where ρ and μ are the density and viscosity of the liquid respectively. Substituting V_r , V_θ and their derivatives from Eqs. 3 and 4 into Eq. 5 yields

$$\frac{\partial P}{\partial r} = \rho U^2\left[\cos^2\theta\left(\frac{a^6}{r^7}-\frac{a^3}{r^4}\right)+\sin^2\theta\left(\frac{3}{2}\frac{a^3}{r^4}+\frac{3}{4}\frac{a^6}{r^7}\right)\right]-4\mu U\frac{a^3}{r^5}\cos\theta \tag{6}$$

Integrating this equation from $P = P(a,\theta)$ to $P(r,\theta)$, gives

$$P(r,\theta)-P(a,\theta) = \rho U^2\left\{\frac{1}{3}\cos^2\theta\left[\left(\frac{a}{r}\right)^3-\frac{1}{2}\left(\frac{a}{r}\right)^6-\frac{1}{2}\right]-\frac{1}{2}\sin^2\theta\left[\left(\frac{a}{r}\right)^3+\frac{1}{4}\left(\frac{a}{r}\right)^6-\frac{5}{4}\right]\right\}$$
$$+\mu U\cos\theta\left[\frac{a^3}{r^4}-\frac{1}{a}\right] \tag{7}$$

The appearance of the viscosity in this equation is in conformity with the viscosity hypothesis advocated by Milne-Thomson [6] (p. 634) although we have inserted inviscid velocity components into the equation of motion.

As $r \longrightarrow \infty$, the pressure $P(r,\theta) \longrightarrow P_\infty$ which is due to the dynamics of the flow , hence Eq. 7 becomes

$$P(a,\theta)-P_\infty = \rho U^2\left[\frac{1}{6}\cos^2\theta-\frac{5}{8}\sin^2\theta\right]+\frac{\mu}{a}U\cos\theta \tag{8}$$

This and the above equation give the pressure distribution on the frontal surface of the spherical – cap bubble.

If one defines $(Cp)_f = \left(P(a,\theta)-P_\infty\right)/0.5\rho U^2$ as the pressure coefficient at the frontal stagnation point where $\theta = 0$, then from Eq. 8 we obtain

$$(Cp)_f = \frac{1}{3} + \frac{4}{\mathrm{Re}^*}$$

(9)

where

$$\mathrm{Re}^* = 2aU/\upsilon$$

3. The Wake Region of the Bubble

Many authors considered the base of the spherical-cap bubble as a flat surface. This will make the pattern of the flow analogous to that behind a circular disk (Kendoush [7]). Assume the center of the circular base of the bubble to be the origin of the cylindrical coordinates R, β, Z. The velocity potential of the circular disk was given by Sparrow and Geiger [8] as follows

$$\Phi = \Phi_1 + \Phi_2$$

(10)

where

$$\Phi_1 = -\left(\frac{2U_w}{\pi}\right)\sqrt{b^2 - R^2}$$

and

$$\Phi_2 = \Phi_2(Z)$$

where Z is the axial coordinate (aligned with U_w). Note that $b = a\sin\theta_m$ and U_w is the main reverse velocity of the wake. The main assumption of using Eq. 10 as the velocity potential of the flow at the wake arises from the similarity in pattern to that of the upstream side as shown in Fig. 2. This assumption has been used with success by the author in the treatment of the sphere hydrodynamics (Kendoush [9]) and the convective heat and mass transfer to the sphere (Kendoush [10]). An example on the verity of this assumption is the streamlines obtained from the numerical solution of Fromm and Harlow [11].

The radial velocity component of the reversed flow of the wake is obtained according to the following

$$V_R = \frac{\partial\Phi}{\partial R} = -\left(\frac{2U_w}{\pi}\right)\left(\frac{R}{b}\right)\left(1-\left(\frac{R}{b}\right)^2\right)^{-\frac{1}{2}} \tag{11}$$

The equation of motion in cylindrical coordinates is

$$\rho V_R \frac{\partial V_R}{\partial R} = -\frac{\partial P}{\partial R} + 2\mu\frac{\partial^2 V_R}{\partial R^2} + \frac{2\mu}{R}\left(\frac{\partial V_R}{\partial R} - \frac{V_R}{R}\right) \tag{12}$$

Substituting V_R and its derivatives from Eq. 11 into Eq. 12 give

$$\left(\frac{\partial P}{\partial R}\right)_w = \left(\frac{12\mu U_w b^2}{\pi}\right)\left(b^2 - R^2\right)^{-\frac{5}{2}} + \left(\frac{4\mu U_w b^2}{\pi R}\right)\left(b^2 - R^2\right)^{-\frac{3}{2}} - \left(\frac{4\mu U_w}{\pi R}\right)\left(b^2 - R^2\right)^{-\frac{1}{2}} - \left(\frac{4\rho {U_w}^2 b^2 R^2}{\pi}\right)\left(b^2 - R^2\right)^{-2}$$

(13)

4. Skirt Formation

The skirt is a very thin envelope of gas trailing the spherical-cap bubble. It originates from the bubble rim and extends downstream the bubble as shown in Fig. 3. Many theories were presented for the explanation of this phenomenon.

Shoemaker and Dechazel [12] related it to a trailing vortex. Guthrie and Bradshaw [13] proposed a theoretical model based on circulation of gas in the skirt envelope. In what follows a logical basis is presented for the skirt formation. If the pressure coefficient of the wake is defined as $(Cp)_w = \left(P(R) - P_w / 0.5\rho U_w{}^2\right)$ where P_w is the pressure at the rear stagnation point, then integrating Eq. 13 yields the following

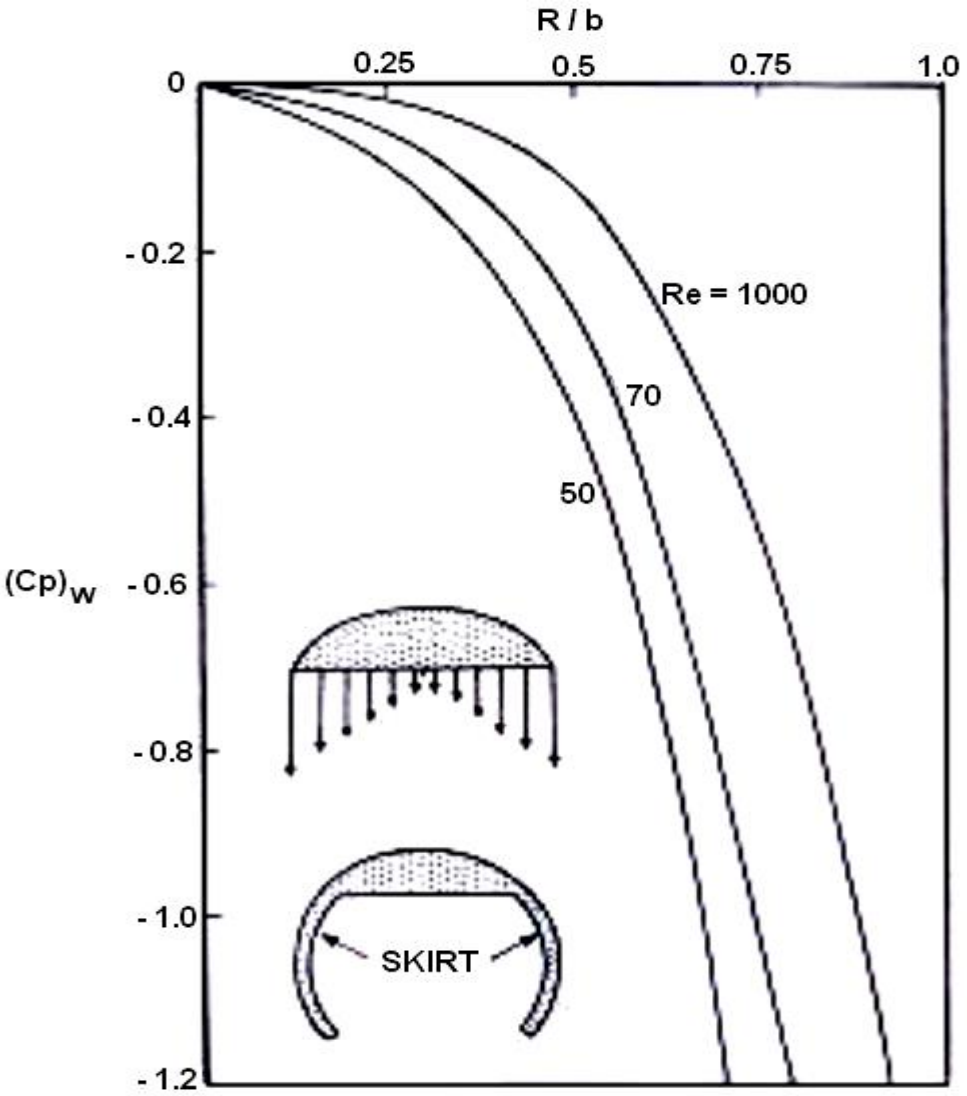

Fig. 3: Pressure distribution on the basal surface of the bubble at different Re numbers

$$(Cp)_w = \left(\frac{16}{\pi \mathrm{Re}^*}\right)\left[2 - \left(1 - \left(\frac{R}{b}\right)^2\right)^{-\frac{3}{2}} - \left(1 - \left(\frac{R}{b}\right)^2\right)^{-\frac{1}{2}}\right] + \frac{4}{\pi^2}\left(\frac{R}{b}\right)^2 \tag{14}$$

Another version of this equation is given in the Appendix. Eq. 14 is illustrated in Fig. 3 after Re_w^* is changed through the following discussion into Re^*.

Lindt [14] found experimentally that the ratio $U_w/U = 0.2$ for $2000 < \mathrm{Re} < 5000$. Narayanan, Goossens and Kossen [15] also found experimentally that this ratio was equal to 0.15 for $7 < \mathrm{Re} < 80$. This means that $\mathrm{Re}_w^* = 0.2\sin\theta_m\,\mathrm{Re}^*$ for Lindt's ratio and $\mathrm{Re}_w^* = 0.15\sin\theta_m\,\mathrm{Re}^*$ for Narayanan et al.'s ratio. When the characteristic length in Re_w^* is changed from $2b$ to $2r_e$ and r_e is the equivalent radius and since $a = 2.2r_e$ then $\mathrm{Re}_w^* = 0.456\sin\theta_m\,\mathrm{Re}$ for Lindt's ratio, noting that $\mathrm{Re} = 2r_eU/\upsilon$. Since $\theta_m = 50^\circ$ for $\mathrm{Re} > 50$, hence $\mathrm{Re}^* = 0.3493\mathrm{Re}$ for Lindt's ratio. Similarly, $\mathrm{Re}^* = 0.342\sin\theta_m\,\mathrm{Re}$ for Narayanan et al.'s ratio.

Fig. 3 offers a logical argument for the skirt formation. The suction pressure in the basal surface of the bubble increases in large proportions near the rim of the bubble causing the gas inside the bubble to be drawn downstream thus forming the skirt. This process will be enhanced in fluids with low surface tension.

5. Discussion and Validation of Theory

Davies and Taylor [16] presented experimental data on the pressure distribution over solid models similar in shape to the spherical-cap bubble. The results were given in terms of the pressure coefficient $Cp^* = \left(P(a,\theta) - P_0\right)/0.5\rho U^2$, where P_0 is the pressure at the forward stagnation point. The prediction of these data necessitates the application of the equation of motion in spherical coordinates, thus

$$\rho\left[\frac{V_rV_\theta}{r} + V_r\frac{\partial V_\theta}{\partial r} + \frac{V_\theta}{r}\frac{\partial V_\theta}{\partial\theta}\right] = -\frac{\partial P}{r\partial\theta} + \frac{2\mu}{r}\frac{\partial}{\partial\theta}\left(\frac{1}{r}\frac{\partial V_\theta}{\partial\theta} + \frac{V_r}{r}\right) + \frac{\partial}{\partial r}\left[\mu\left(r\frac{\partial}{\partial r}\left(\frac{V_\theta}{r}\right) + \frac{1}{r}\frac{\partial V_r}{\partial\theta}\right)\right]$$
$$+ \frac{2\mu}{r}\left(\frac{1}{r}\frac{\partial V_\theta}{\partial\theta} - \frac{V_\theta\cot\theta}{r}\right)\cot\theta + \frac{3\mu}{r}\left(r\frac{\partial}{\partial r}\left(\frac{V_\theta}{r}\right) + \frac{1}{r}\frac{\partial V_r}{\partial\theta}\right) \tag{15}$$

Substituting V_r, V_θ and their derivatives from Eqs. 3 and 4 into Eq. 15 after evaluating the terms at the surface of the bubble and the integrating yields

$$\int_{P_o}^{P(a,\theta)} dP = \frac{3\mu U}{2}\int_0^\theta \frac{\cos^2\theta}{\sin\theta}\,d\theta - \frac{9\rho U^2}{4}\int_0^\theta \sin\theta\cos\theta d\theta \tag{16}$$

A singularity arises from evaluating the first integral on the right side of Eq. 15. This was mitigated by expanding the integrand ($\cos^2\theta/\sin\theta$) in a Taylor series about the angle $\theta = 0.1\theta_m$. Retention of the first two terms of the series gives after performing some algebra

$$\left(C_P^*\right)_f = \left(\frac{6}{\mathrm{Re}^*}\right)\left(22.9341\theta - 66.1879\theta^2\right) - \left(\frac{9}{4}\right)\sin^2\theta \tag{17}$$

The Reynolds number Re^* was calculated from the data of Davies and Taylor [16] and was found to be 50238. Fig. 4 shows a good agreement between Eq. 17 and the experimental and theoretical results of Davies and Taylor [16].

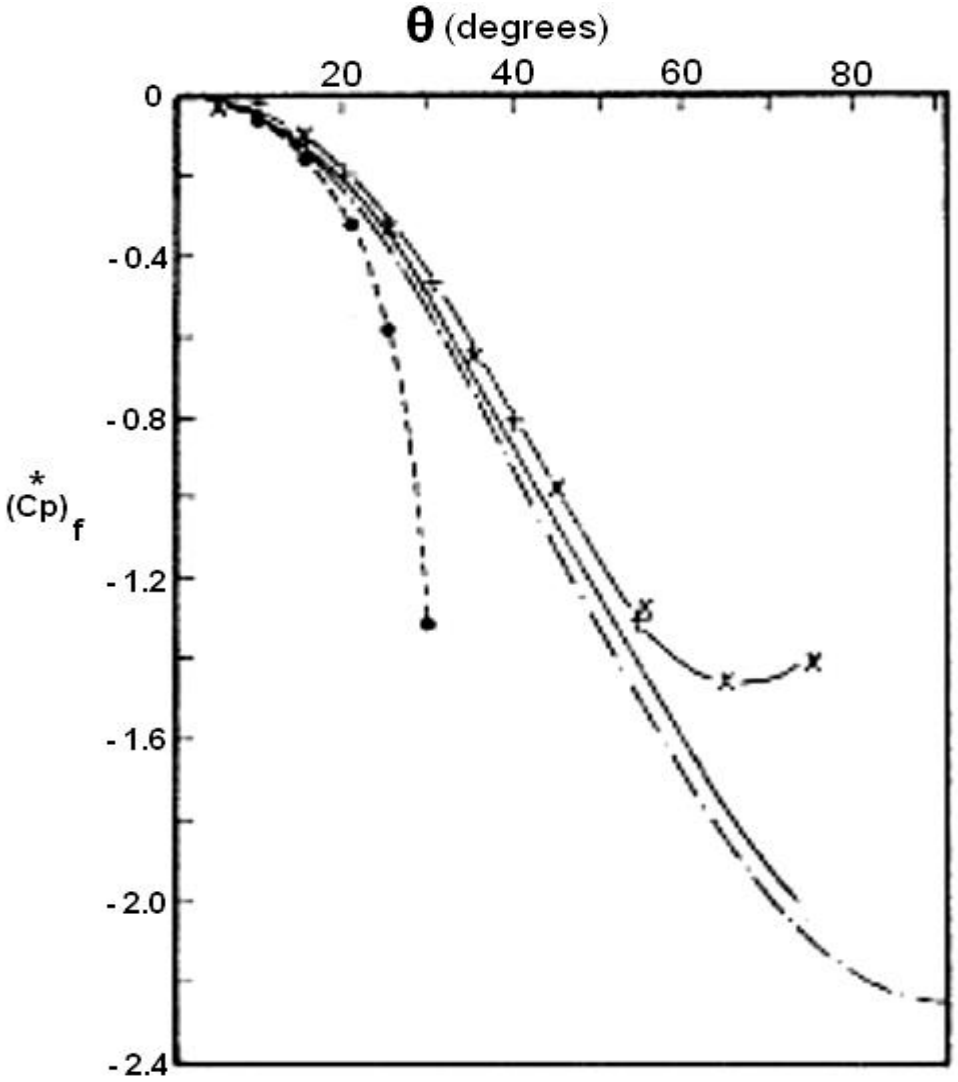

Fig. 4: Comparison with the experimental and theoretical results of Davis and Taylor [16] : (• • •) $\theta_m = 30$; (+ + +) $\theta_m = 55$; (x x x) $\theta_m = 75$; (▬ · ▬ · ▬); Theoretical curve for a sphere and (_____) present Eq. 17, $\mathrm{Re} = 50238$.

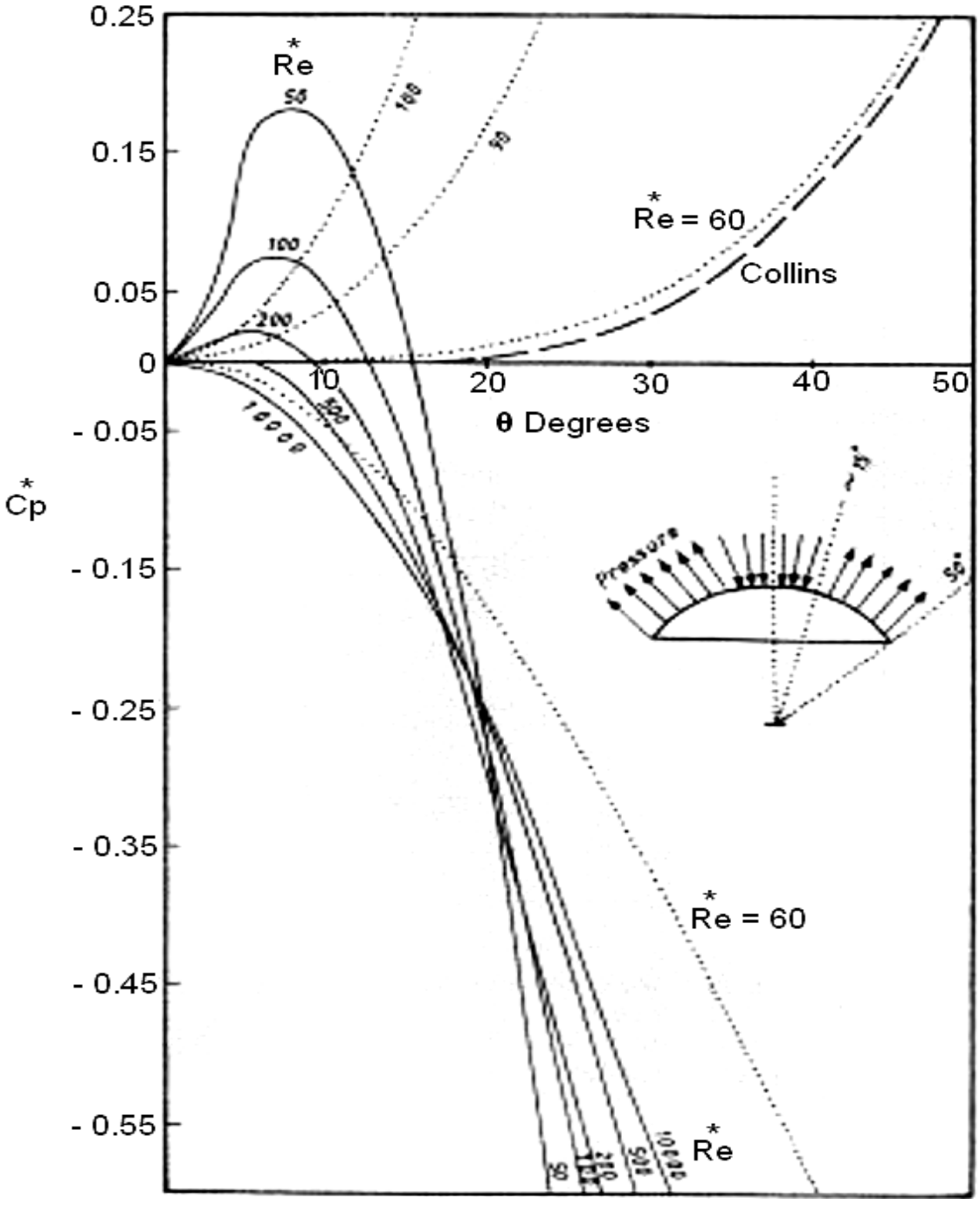

Fig. 5: Pressure distribution on the frontal surface of the bubble. (_____) Present solution; (__ __ __) Collins [4]; Wairegi and Grace [17]; ($M = 7.16x10^{-3}$, $W = 40$).

Another comparison is shown in Fig. 5 between Eq. 17, the theoretical solution of Collins [4] and the equation of Wairegi and Grace [17] which was quoted in the book of Clift, Grace and Weber [18] (p. 205) as

$$P(a,\theta) - P_o = ag\rho(1-\cos\theta) - \left(\frac{9}{8}\right)\rho U^2 \sin^2\theta \tag{18}$$

The above equation was made dimensionless so that it will be compatible with the present terminology as follows

$$C_p^* = \left([1-\cos\theta] \frac{M\,\mathrm{Re}^{*4}}{We^3} \right) - \left(\frac{9\sin^2\theta}{4} \right) \tag{19}$$

where

M is Morton number $= 7.16x10^{-3}$

We is Weber number $= 40$

The above equation was derived on the basis of Bernoulli's theorem that implies that viscous forces were insignificant. Contrary to the present results, Collins [4] and Wairegi and Grace [17] predicted high positive pressure at the bubble rim, which would oppose the tendency of skirt formation.

Miksis, Vanden-Broeck and Keller [19] utilized the theoretical derivation of Moore [20] for the pressure across the boundary layer over the frontal surface of the spherical bubble, which is given as follows†

$$P_{BL}(\theta) = 12\rho U^2 \frac{\left[\left(\frac{2}{3}\right) - \cos\theta - \left(\frac{1}{3}\right)\cos^3\theta \right]}{\mathrm{Re}^* \sin^3\theta} \tag{20}$$

The normal viscous stress around the bubble was obtained from the potential flow as follows

$$\sigma_{rr}(\theta) = \frac{12\rho U^2 \cos\theta}{\mathrm{Re}^*} \tag{21}$$

Based on the above relations, Miksis et al.[19] concluded that the ratio

$$\frac{P_{BL}(\theta)}{\sigma_{rr}(\theta)} \le 0.31 \quad \text{for } \theta = 0 \text{ to } \theta = 45^\circ$$

Eq. (17) may be written in the following form

$$P(\theta) - P_o = \left(\frac{3\rho U^2 \left(22.9341\theta - 66.1879\theta^2\right)}{\mathrm{Re}^*} \right) - \frac{9}{8}\rho U^2 \sin^2\theta \tag{22}$$

This equation is analogous to Eq. 20 which is originally due to Moore [20] as both equations describe the angular distribution of the pressure on the frontal surface of the bubble. The ratio of this equation to Eq. 21 yields

$$\frac{P(\theta) - P_o}{\sigma_{rr}(\theta)} = \frac{\left[3\left(22.9341\theta - 66.1879\theta^2\right) - 0.375\mathrm{Re}^* \sin^2\theta\right]}{4\cos\theta} \tag{23}$$

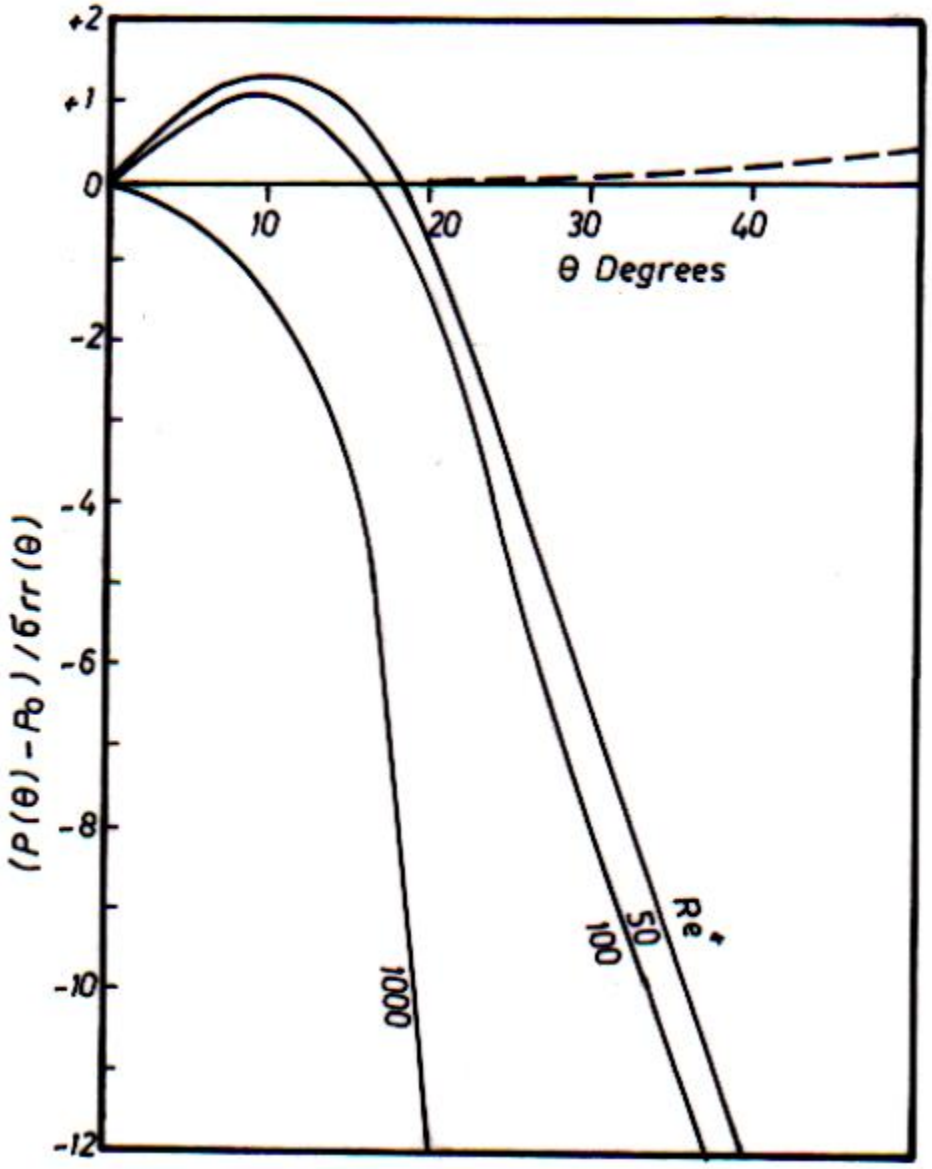

Fig. 6: A comparison between the ratio of the angular pressure distribution to the normal stress of Miksis et al. [19] (__ __ __) and the present ratio (Eq. 23) (_____).

Fig. 6 shows a comparison between the ratio of Miksis et al. [19] and the above ratio, which indicates clearly that the conclusion of Miksis et al.[19] mentioned earlier was not precise. The present ratio (that is, Eq. 23) seems more comprehensive as it gives a functional dependence on Reynolds number as well as the angular position. Note that, there is typographic error in Miksis et al.'s paper. The exponent of $(1/3)\cos\theta$ should be 3 instead of 2.

6. CONCLUSIONS

A method of calculating the pressure field around the spherical-cap bubble has been presented. This method divides the field into two distinct regions, a frontal and a wake region. Two irrotational inviscid flow models were used one for the front and the other for the wake. These models were incorporated into the equation of motion. The resulted pressure coefficient equations were compared favourably with the available theoretical and experimental data.

APPENDIX

Another version of the pressure coefficient

Integrating Eq. 13 starting from $R \longrightarrow \infty$ where the pressure is P_∞ to any radial position on the surface of the circular base of the cap and adopting a pressure coefficient for the wake region yields

$$\left(C_p\right)_w^* = \frac{\left(P(R) - P_\infty\right)}{0.5\rho U_w^2} = \frac{16}{\pi \,\mathrm{Re}_w^*}\left[\frac{b^3}{R^3}\left(\frac{b^2}{R^2}-1\right)^{-\frac{3}{2}}\right] + \frac{16}{\pi \,\mathrm{Re}_w^*}\left[\frac{b}{R}\left(\frac{b^2}{R^2}-1\right)^{-\frac{1}{2}}\right] - \frac{4}{\pi^2}\left(\frac{b}{R}\right)^2\left(\frac{b^2}{R^2}-1\right)^{-1}$$

(A1)

where

$\mathrm{Re}_w^* = 2bU_w\rho/\mu$

References

[1] Wegener, P.P. and Parlange, J.-Y., "Spherical-Cap Bubbles," *Ann. Rev. Fluid Mech*., vol. 5, pp. 79-100, 1973.

[2] Kendoush, A.A., "Theory of Convective Heat and Mass Transfer to Spherical-Cap Bubbles," *AIChE Journal*, vol. 40, pp. 1445-1448, 1994.

[3] Maxworthy, T., Gnann C., Kurten M. and Durst, F., "Experiments on the Rise of Air Bubbles in Clean Viscous Liquids," *J. Fluid Mech*., vol. 321, pp. 421-441, 1996.

[4] Collins, R., "A Second Approximation for the Velocity of a Large Gas Bubble Rising in an Infinite Liquid," *J. Fluid Mech*., vol. 25, pp. 469-480,1996.

[5] Lazarek, G.M. and Littman, H., "The Pressure Field due to a Large Circular-Capped Air Bubble," *J. Fluid Mech*., vol. 66, pp. 673-687, 1974.

[6] Milne-Thomson, L.M., *Theoretical Hydrodynamics*, 5th Ed., Macmillan, London, 1972.

[7] Kendoush, A.A., "Hydrodynamics and Heat Convection from a Disk Facing a Uniform Flow," ASME Summer Conference, 2004, Paper No. HT-FED 2004-56797.

[8] Sparrow, E.M. and Geiger G.T., "Local and Average Heat Transfer Characteristics for a Disk Situated Perpendicular to a Uniform Flow, " *J. Heat Transfer*, vol. 107, pp. 321-326, 1985.

[9] Kendoush, A.A., "Calculation of Flow Resistance from a Spherical Particle," *Chem. Eng. Process*, vol. 39, pp. 81-86, 2000.

[10] Kendoush, A.A., "Low Prandtl Number Heat Transfer to Fluids Flowing Past an Isothermal Spherical Particle," *Int. J. Heat and Fluid Flow*, vol. 16, pp. 291-297,1995.
[11] Fromm, J.E. and Harlow, F.H., "Numerical Solution of the Problem of Vortex Street Development," *Phys. Fluids*, vol. 6, pp. 975-982, 1963.
[12] Shoemaker, P.D. and DeChazal, L.M.E., "Dimpled and Skirted Drops Moving through Viscous Liquid Media," *Chem. Eng. Sci.*, vol. 24, pp. 795-797, 1969.
[13] Guthrie, R.I.L. and Bradshaw, A.V., "The Stability of Gas Envelopes Trailed behind Large Spherical-Cap Bubbles Rising through Viscous Liquids," *Chem. Eng. Sci*., vol. 24, pp. 913-917, 1969.
[14] Lindt, J.J., "Note on the Wake behind a Two-Dimensional Bubble," *Chem. Eng. Sci.*, vol. 26, pp. 1776-1777, 1971.
[15] Narayanan, S., Goossens, L.H.J. and Kossen, N.W.F., "Coalescence of Two Bubbles Rising in Line at Low Reynolds Numbers," *Chem. Eng. Sci.*, vol. 29, pp. 2071-2082,1974.
[16] Davies, R. and Taylor, G.I., "The Mechanics of Large Bubbles Rising through Extended Liquids and through Liquids in Tubes," *Proc. Roy. Soc. London*, vol. A200, pp. 375-590, 1950.
[17] Wairegi, T. and Grace, J.R., "The behaviour of large drops in immiscible liquids," *Int. J. Multiphase Flow*, vol. 3, pp. 67-77. 1976.
[18] Clift, R., Grace, J.R. and Weber, M.E., *"Bubbles, Drops and Particles,"* Academic press, New York, 1978.
[19] Miksis, M.J., Vanden-Broeck, J.-M. and Keller, J.B., "Rising Bubbles," *J. Fluid Mech*., vol. 123, pp. 31-41,1982.
[20] Moore, D.W., "The Boundary Layer on a Spherical Bubble," *J. Fluid Mech.*, vol. 16, pp. 161-176, 1963.